ISSN No: 2348-4845
International Journal & Magazine of Engineering, Technology, Management and Research
A Peer Reviewed Open Access International Journal

Adjustable Frequency–Duty-Cycle Hybrid Control Strategy for Full-Bridge Series Resonant Converters in Electric Vehicle Chargers

S.Sai Krishna
M.Tech Student
Department of EEE,
Visvodaya Engineering College,
Kavali, S P S R NELLOER,
AP, India-524201.

A.Bhaktha Vachalaa
Associate Professor
Department of EEE,
PBR VITS,
S P S R NELLOER,
AP, India-524201.

Abstract:

In this paper, an effective output voltage control method using adjustable frequency–duty-cycle hybrid control is presented. By using the proposed method, the operating performance of the full-bridge series resonant dc–dc converter applied to the onboard charger in electric vehicles under the constant-voltage charge mode is improved. The proposed control method improves the system efficiency of the charger up to 4% for light load conditions compared with the conventional control method without any extra hardware. A theoretical analysis is described along with a loss analysis in detail, and the validity of the proposed method is verified by experiment with a 3.3-kW prototype onboard charger.

1. Introduction:

For the onboard charger (OBC) installed in plug-in hybrid electric vehicles (EVs) and pure EVs, high efficiency and high power density are required to maximize the energy utilization and the distance covered per charge. Using resonant converters capable of soft switching at a high switching frequency is an effective solution for these requirements. In this regard, various converter topologies such as series, parallel, and LLC resonant converters are being actively adopted on the dc–dc converter for the OBC in EVs. Among the various charge algorithms for Li-ion batteries in EVs, it is known that the constant-current (CC) and constant-voltage (CV) charge methods are effective and widely applied to the charger. In the first charging phase, the battery voltage is gradually increased at a constant current. As soon as the battery voltage reaches the trickle level, the CV charge method is applied as the charging current gradually drops to the maintenance level. It should be noted here that the CV charge mode controls the low–medium load range, and its charge time is almost about 40% of the total charge time. Therefore, the efficiency during the CV charge mode should be improved for higher energy utilization. For example, in general, a 3.3-kW prototype OBC with a maximum efficiency of 93% could be accomplished by using a full-bridge series resonant dc–dc converter with the CC–CV charge algorithm. Unfortunately, this type of charger has less than 84% efficiency under light load conditions less than 500 W. Moreover, operation near 300 W is unstable and not well controlled. This is because the output voltage of the full bridge series resonant dc–dc converter is controlled by only adjusting the switching frequency. According to the impedance variation of the Li-ion battery, the switching frequency sharply increases from full load to light load so that the switching losses increase,

ISSN No: 2348-4845
International Journal & Magazine of Engineering, Technology, Management and Research
A Peer Reviewed Open Access International Journal

resulting in deteriorated system performance. In the case of a phase-shifted full-bridge converter for an OBC it cannot ensure zero voltage switching (ZVS) operation at light loads because of the limitations of the leakage inductance. Further, the effective duty cycle for transferring power is reduced because the switching frequency is fixed for the entire load range. This power reduction results in a reduction of the efficiency of the converter for light loads. In the previous research, to alleviate the problems of ZVS in the phase-shifted full-bridge converter, a full-bridge resonant converter with a modified resonant network has been studied .On the other hand, the use of pulse width modulation technologies instead of conventional frequency modulation technology to improve the efficiency of the resonant converter have been studied. However, in previous works, only the duty cycles are changed with fixed switching frequency to control the output voltage of the half-bridge dc–dc converter. As a result, the converter cannot be operated under ZVS condition owing to the limitations of the duty cycle, leading to a decrease in the efficiency for light loads. Thus, an effective control method that allows the OBC to carry out soft switching for a wide range of loads is required.

2. Literature Survey:

A. Kuperman, U. Levy, J. Goren, A. Zafransky, and A. Savernin, are proposed that this paper presents the functionality of a commercialized fast charger for a lithium-ion electric vehicle propulsion battery. The device is intended to operate in a battery switch station, allowing an up-to 1-h recharge of a 25-kWh depleted battery, removed from a vehicle. The charger is designed as a dual-stage-controlled ac/dc converter. The input stage consists of a three-phase full-bridge diode rectifier combined with a reduced rating shunt active power filter. The input stage creates an uncontrolled pulsating dc bus while complying with the grid codes by regulating the total harmonic distortion and power factor according to the predetermined permissible limits. The output stage is formed by six interleaved groups of two parallel dc-dc converters, fed by the uncontrolled dc bus and performing the battery charging process. The charger is capable of operating in any of the three typical charging modes: constant current, constant voltage, and constant power. Extended simulation and experimental results are shown to demonstrate the functionality of the device.

A. Hajimiragha, C. A. Cañizares, M. W. Fowler, and A. Elkamel are proposed that this paper analyzes the feasibility of optimally utilizing Ontario's grid potential for charging plug-in hybrid electric vehicles (PHEVs) during off-peak periods. Based on a simplified zonal model of Ontario's electricity-transmission network and a zonal pattern of base-load generation capacity from 2009 to 2025, an optimization model is developed to find the optimal, as well as maximum, penetrations of PHEVs into Ontario's transport sector. The results of this paper demonstrate that the present and projected electricity grid in Ontario can be optimally exploited for charging almost 6% of the total vehicles in Ontario or 12.5% of the vehicles in Toronto's transport sector by 2025; this corresponds to approximately 500 000 PHEVs that can be charged from the grid without any additional transmission or power-generation investments beyond those currently planned.

M. Yilmaz and P. T. Krein are proposed the current status and implementation of battery chargers, charging power levels, and infrastructure for plug-in electric vehicles and hybrids. Charger systems are categorized into off-board and on-board types with unidirectional or bidirectional power flow. Unidirectional charging limits hardware requirements and simplifies interconnection issues. Bidirectional charging supports battery energy injection back to the grid. Typical on-board chargers restrict power because of weight, space, and cost constraints. They can be integrated with the electric drive to avoid these problems. The availability of charging infrastructure reduces on-board energy storage requirements and costs. On-board charger systems can be conductive or inductive. An off-board charger can be designed for high charging rates and is less constrained by size and

ISSN No: 2348-4845
International Journal & Magazine of Engineering, Technology, Management and Research
A Peer Reviewed Open Access International Journal

weight. Level 1 (convenience), Level 2 (primary), and Level 3 (fast) power levels are discussed. Future aspects such as roadbed charging are presented. Various power level chargers and infrastructure configurations are presented, compared, and evaluated based on amount of power, charging time and location, cost, equipment, and other factors.

M. G. Egan, D. L. OSullivan, J. G. Hayes, M. J. Willers, and C. P. Henze, are proposed a novel power-factor-corrected single-stage alternating current/direct current converter for inductive charging of electric vehicle batteries is introduced. The resonant converter uses the current-source characteristic of the series-parallel topology to provide power-factor correction over a wide output power range from zero to full load. Some design guidelines for this converter are outlined. An approximate small-signal model of the converter is also presented. Experimental results verify the operation of the new converter

J. Y. Lee and H. J. Chae,aresuggests another candidate for high-power onboard charger for electric vehicles. It is based on a discontinuous conduction mode (DCM) power factor correction (PFC) converter with harmonic modulation technique that improves the power factor in DCM PFC operation and a two-stage dc/dc converter composed of a resonant converter and a DCM buck converter. Separating the functions of the dc/dc stage into control and isolation helps to reduce the transformer by using high-frequency resonance. The feasibility of the proposed charger has been verified with a 6.6-kW prototype.

3. Proposed System

This paper discusses an adjustable frequency–duty-cycle (AFDC) hybrid control method in which the duty cycle and the switching frequency are adjusted according to load variations to control the output voltage. Moreover, the effective duty cycles and switching frequencies for the optimum operating points that ensure soft switching are induced. The proposed method improves the operating performance of the OBC in EVs under light loads without additional hardware. Based on the analytical results, accurate duty cycles available for ZVS operation are estimated for load variations. Then, the loss analyses of the major components such as semiconductors, the transformer, and the resonant inductor are performed. Finally,the overall performance of the proposed control method is verified by experiment with a 3.3-kW prototype OBC.

A. Operational Characteristics of AFDC Hybrid Control

To compensate the performance degradation problem under light loads in the CV charge mode, the switching frequency should be reduced. As shown in Fig. 1(b) and (1), the inputto-output voltage gain can be characterized by dividing the ac equivalent resistance Rac by the total impedance of the resonant network Zin. Zin increases with an increase in the switching

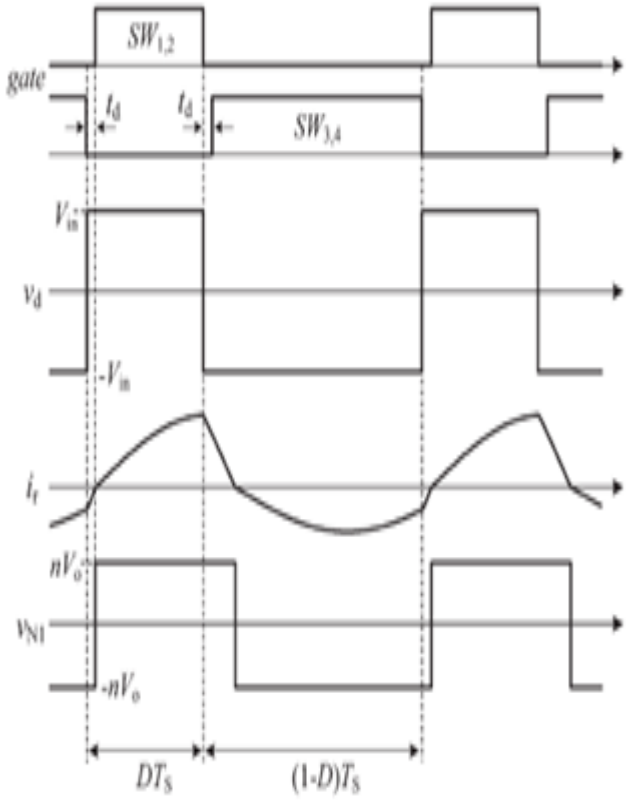

Fig. 3. Steady-state operating waveforms of AFDC hybrid control. Frequency above the resonance frequency.

ISSN No: 2348-4845
International Journal & Magazine of Engineering, Technology, Management and Research
A Peer Reviewed Open Access International Journal

Under conventional frequency control with D = 0.5, the RMS value of the square wave voltage applied to the resonant network is constant. Therefore, Zin should increase according to the load reduction to maintain the voltage ratio at a constant value. Implicit in this voltage relationship is the fact that the output voltage can be maintained constant provided the value of the total impedance and the RMS value of the square-wave input voltage of the resonant network are appropriately adjusted according to the load reduction. The main concept of the proposed AFDC hybrid control is as follows. The RMS value of the square-wave input voltage of the resonant network can be reduced by changing the duty cycle. On the other hand, the value of the total impedance can be minimized by reducing the switching frequency because the resonant network impedance is a function of the switching frequency. This implies that the converter can be operated at lower switching frequencies than the switching frequencies of the conventional control method for light loads. Thus, it is important to analyze the relationship between the duty cycle and the switching frequency for efficient operation of the converter. Fig. 3 shows the steady-state operating waveforms of the converter by AFDC hybrid control for an arbitrary CV charge mode. In the operating waveforms in Fig. 3, the time variation and the phase of the hth-order harmonic of vdare respectively given by

$$v_d(t) = V_{in}(2D-1) + \sum_{h=1}^{\infty} 2\sqrt{2} \times \left[\frac{V_{in}}{h\pi}\sqrt{1-\cos(2\pi h D)}\,\sin(h\omega t + \theta_h)\right] \quad (3)$$

$$\theta_h = \tan^{-1}\left[\frac{\sin(2h\pi D)}{1-\cos(2h\pi D)}\right]. \quad (4)$$

The dc component of the square-wave voltage vdis blocked by the series resonant capacitor Cr; thus, the ac component of vdforces the resonant current irto flow through the resonant network. The ac component of vdis given by

$$v_{dac}(t) = \sum_{h=1}^{\infty} \frac{2\sqrt{2}V_{in}}{\pi}\left[\frac{1}{h}\sqrt{1-\cos(2\pi h D)}\,\sin(h\omega_s t + \theta_h)\right]. \quad (5)$$

The RMS value of the square-wave voltage, which contributes to the transfer of active power to the load, can be calculated by applying harmonic components. Therefore, the RMS voltage Vdis expressed as

$$V_d = \frac{2V_{in}}{\pi}\sqrt{\sum_{h=1}^{\infty}\left(\frac{1}{h^2}(1-\cos(2\pi h D))\right)}. \quad (6)$$

The secondary-side voltage of the transformer is clamped to the output voltage Vo; hence, the RMS value of the voltage across the ac equivalent resistance in Fig. 1(b) is represented as nVo. The RMS voltage of the resonant network input to the RMS voltage reflected to the primary side is expressed by using Kirchoff's voltage law, i.e.,

$$\frac{n V_o}{V_d} = \frac{R_{ac}}{Z_{in}} \quad (7)$$

whereZin represents the total impedance of the hth-order harmonic of the resonant network, i.e.,

$$Z_{in} = \sqrt{R_{ac}^2 + \frac{L_r}{C_r}\left(h\omega_n - \frac{1}{h\omega_n}\right)^2}. \quad (8)$$

Therefore, the input dc source to the output voltage gain for the proposed AFDC hybrid control is derived by substituting (6) into (7) as follows:

$$\frac{V_o}{V_{in}} = \frac{2R_{ac}}{n\pi}\sqrt{\sum_{h=1}^{\infty}\left(\frac{1}{h^2 Z_{in}^2}(1-\cos(2\pi h D))\right)}. \quad (9)$$

Equation (9) is simplified for the voltage gain of the converter with consideration of the fundamental RMS value by the filtering action of the Lr− Cr resonant network as follows:

$$\frac{V_o}{V_{in}} \cong \frac{2R_{ac}}{n\pi}\,\frac{\sqrt{1-\cos(2\pi D)}}{\sqrt{R_{ac}^2 + \frac{L_r}{C_r}(\omega_n - 1/\omega_n)^2}} = \frac{2\sqrt{2}}{n\pi}\,\frac{\sin(\pi D)}{\sqrt{1+Q^2(\omega_n - 1/\omega_n)^2}}. \quad (10)$$

ISSN No: 2348-4845
International Journal & Magazine of Engineering, Technology, Management and Research
A Peer Reviewed Open Access International Journal

Fig. 4 shows the voltage gains according to the variation in ωnfor various values of D for n = 0.73 at 100% and 30% loads. As shown in Fig. 4, the decrease in the duty cycle reduces the input–output voltage gain at the same frequency.

On the other hand, it is observed that the switching frequency decreases with a reduction of the duty cycle while maintaining the same input–output voltage gain. In particular, the decrease in the switching frequency is distinguishable for light loads. This implies that the decrease in the switching frequency can alleviate the switching losses and eventually enhance the converter efficiency.

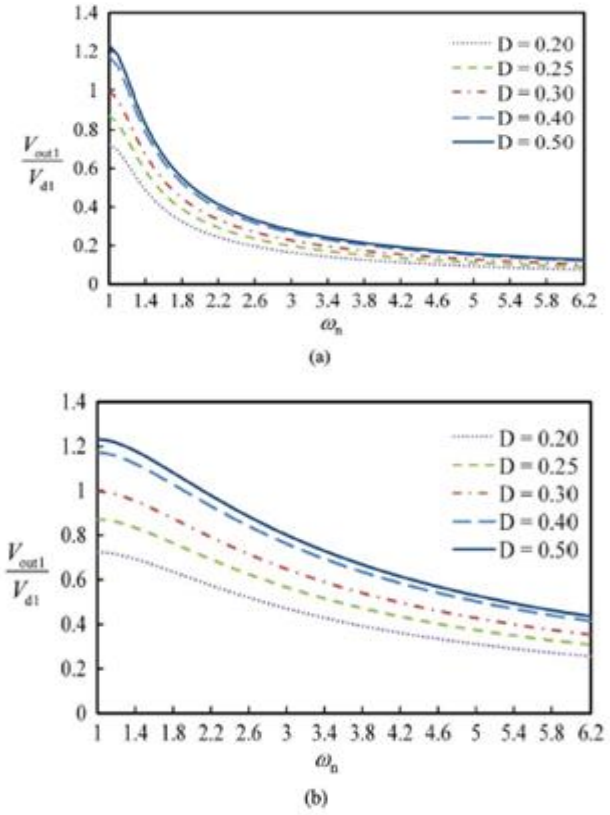

Fig. 4. Voltage gain as a function of ωnfor different duty cycles D. (a) 100% load. (b) 30% load.

The full-bridge series resonant dc–dc converter applied to the developed 3.3-kW prototype OBC has the following specifications: maximum output power Po = 3.3 kW, input dc voltage Vin = 380 V, output voltage Vo = 400 V, resonant inductance Lr= 75 μH, resonant capacitor Cr = 66 nF, and transformer turns ratio n(= N1/N2) = 19/26. Thus, it is necessary to determine the range of duty cycles available for load variations during the CV charge mode. The equation for the useable duty cycle is derived from (10) and is given by

$$D = \frac{1}{\pi}\sin^{-1}\left(\frac{n\pi V_o}{2\sqrt{2}V_{in}}\sqrt{1+Q^2(\omega_n - 1/\omega_n)^2}\right). \quad (11)$$

It is shown in (11) that D is a function of Q and ωnwith the given parameters Vo, Vin, and n. Therefore, D can be expressed according to the frequency variations with respect to each load. Fig. 5 shows the theoretically adjustable duty cycle for Vo= 400 V. As shown in Fig. 5, the switching frequency should be varied by about 4.4 times the resonant frequency to obtain the same output voltage as the load is changed from 100% to 10% for D = 0.5. On the other hand, a smaller duty cycle at the same load means that the switching frequency is smaller. Moreover, It can be seen that the frequency variation is definitely small compared with D = 0.5 as the load changes from 100% to 10%. This implies that the switching frequency can be decreased by reducing the duty cycle because the load is smaller during the CV charge mode. Switching losses can be

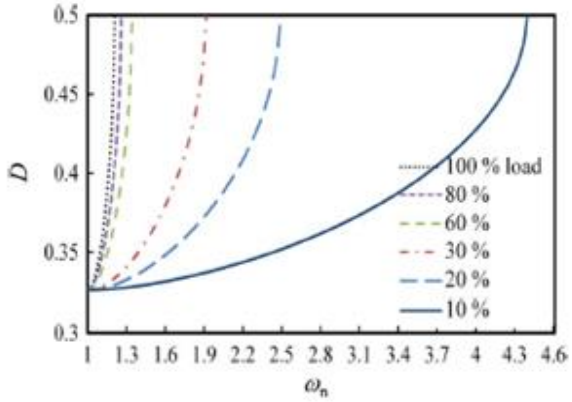

Fig. 5. Theoretically adjustable duty cycles for load variations for the given parameters.

dramatically minimized at turn off by the decreased switching frequencies. Theoretically, the duty cycle can be reduced by a factor of 0.33 to maintain the

ISSN No: 2348-4845
International Journal & Magazine of Engineering, Technology, Management and Research
A Peer Reviewed Open Access International Journal

output voltage at 400 V in the range of loads considered for the developed 3.3-kW prototype OBC.

B. Estimation of the ZVS Operation Range

Guaranteeing the ZVS range is a key aspect for operating resonant converters. Therefore, it is important to estimate the duty cycles corresponding to the switching frequencies that ensure the ZVS range to improve the decreased efficiencies due to increased switching frequencies in the CV charge mode. During operation, each of the fundamental and harmonic voltage components given by (5) produces fundamental and harmonic currents through the series resonant network. In conventional frequency control with D = 0.5, the positive resonant current flowing through the resonant network is always symmetrical to the negative resonant current because the phase of the fundamental voltage is in phase with that of the hth-order harmonic voltage. This implies that each switch is turned off under the same current conditions. As shown by (4), however, the phases of the fundamental and harmonic voltages vary according to D. This is different from the hth-order harmonics and leads to an asymmetrical resonant current. Accordingly, switches (SW1−SW4) are turned off under different current conditions. The time-varying resonant current through the resonant networks derived from (5) and given by

$$i_r(t) = \sum_{h=1}^{\infty} \frac{2\sqrt{2}V_{in}}{\pi}\left[\frac{1}{hZ_{in}}\sqrt{1-\cos(2\pi hD)} \times \sin(h\omega_s t + \theta_h - \varphi_h)\right] \quad (12)$$

whereϕh represents the phase delay of the hth-order harmonic between vdac and ir, as given by

$$\varphi_h = \tan^{-1}\left[Q\left(h\omega_n - \frac{1}{h\omega_n}\right)\right]. \quad (13)$$

Normally, the condition for ZVS operation in all switches is represented from (4) and (13) as follows [14]:

$$\Delta\phi = \varphi_1 - \theta_1 > 0 \quad (14)$$

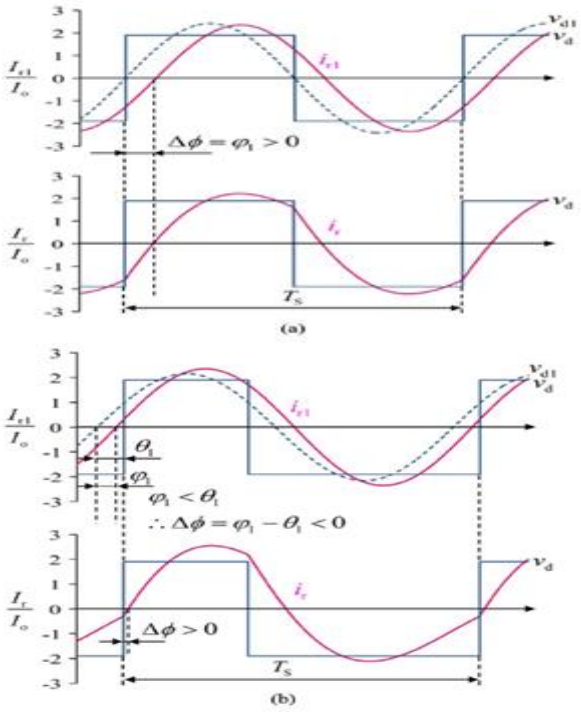

Fig. 6. Phase delay between vdand ir. (a) D = 0.5. (b) D = 0.35.

whereϕ1 is the phase delay between the fundamental voltage of vdand the fundamental current of ir, and θ1 is the phase of the fundamental voltage of vd. To satisfy (14), ϕ1 should increase as the load decreases, Under the traditional frequency control method with D = 0.5, θ1 is zero by using (4). However, θ1 is inversely proportional to D. On the other hand, ϕ1 does not depend on D but proportional to the switching frequency. In Fig. 6, the fundamental resonant current normalized by the maximum power output current using the fundamental component of the square-wave input voltage is compared with the realistic resonant current by harmonic synthesis to achieve the desired value of the output voltage at an arbitrary load. As shown in Fig. 6, there is little difference in the phase delay between the fundamental current and the realistic current at D = 0.5. When D = 0.35, the difference in the phase delay between both currents is evident. Furthermore, converter designers may make errors by concluding rashly that ZVS cannot be achieved forD<0.35 when estimating the ZVS conditions for loads with (14). Thus, it is necessary to use the fundamental component and hth-order harmonic

ISSN No: 2348-4845
International Journal & Magazine of Engineering, Technology, Management and Research
A Peer Reviewed Open Access International Journal

components for more exact analysis for asymmetrical duty cycle control, particularly when investigating the ZVS range.

As can be seen from the steady-state operating waveforms, the current of switches SW1 and SW2 at turn off causes the antiparallel diodes of switches SW3 and SW4 to conduct prior to the turn on of SW3 and SW4. Similarly, the operation of switches SW1 and SW2 is caused by the turn off of switches SW3 and SW4. Consequently, the turn-off currents provide information on whether the switches (SW1 − SW4) are turned on under ZVS conditions [9]. The values of currents ISW1, 2 and ISW3, 4 are defined at DTS and TS, respectively, and are given by

$$I_{SW_{1,2}} = \sum_{h=1}^{\infty} \frac{2\sqrt{2}V_{in}}{\pi} \left[\frac{1}{hZ_{in}} \sqrt{1-\cos(2\pi hD)} \times \sin(2\pi hD + \theta_h - \varphi_h) \right] \quad (15)$$

$$I_{SW_{3,4}} = \sum_{h=1}^{\infty} \frac{2\sqrt{2}V_{in}}{\pi} \left[\frac{1}{hZ_{in}} \sqrt{1-\cos(2\pi hD)} \sin(\theta_h - \varphi_h) \right] \quad (16)$$

$$\text{ZVS Condition for } SW_1 \,\&\, SW_2: \quad I_{SW_{3,4}} < 0 \quad (17)$$

$$\text{ZVS Condition for } SW_3 \,\&\, SW_4: \quad I_{SW_{1,2}} > 0. \quad (18)$$

By energy balance of the resonant network, the value of ISW1, 2 at turn off increases as the turn-on time DTS of switches SW1 and SW2 decreases; thus, switches SW3 and SW4 are sure to be turned on under zero voltage for various loads. In contrast, the absolute value of ISW3, 4 at the end of the switching period TS is smaller. Furthermore, because the drain–source capacitor Coss exists in parallel with the switch, ISW3, 4 should exceed the minimum value necessary to completely charge/discharge Coss within the dead time td to guarantee ZVS. Assuming the overall capacitor Cs(= 2Coss)is in parallel with every switch of the full-bridge converter, the minimum value of ISW3, 4 is defined as

$$|I_{SW_{3,4}}| \geq \frac{C_S V_{in}}{t_d}. \quad (19)$$

Determination of the ZVS ranges of all switches by investigating whether the value calculated from (16) satisfies the necessary requirements of (17) and (19) for various loads is very adequate. Fig. 7 shows the effective duty cycles available for various loads corresponding to each switching frequency for Vo= 400 V during the CV charge mode. As shown in Fig. 7(a) and (b), the analysis using harmonic decomposition offers more exact information about the ZVS ranges. This implies that the turn-off switching losses can be alleviated as the converter is operated along the red dotted line, which indicates the optimum operation points, for various loads.

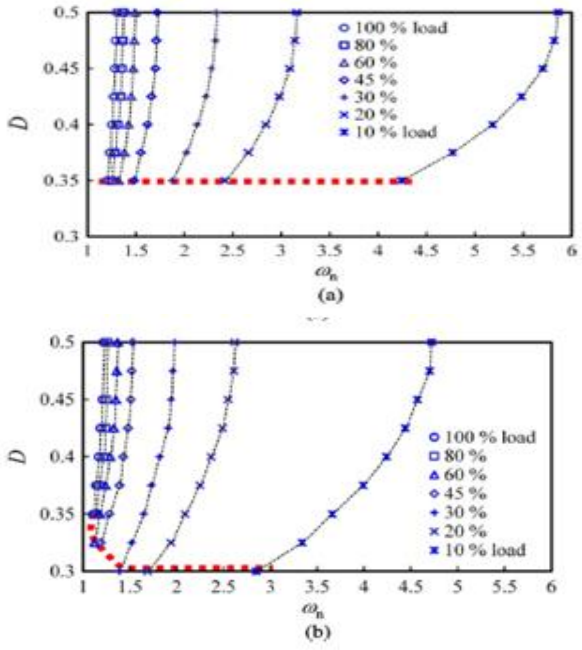

Fig. 7. Effective duty cycles according to load for Vo= 400 V. (a) First harmonic approximation analysis. (b) Harmonic analysis.

IV. LOSS ANALYSIS

Here, a loss analysis is carried out to predict the efficiency. In this paper, the main sources of loss are analyzed, neglecting the parasitic components such as stray inductances and capacitance on the basis of the simulation results and calculated values in the previous

ISSN No: 2348-4845
International Journal & Magazine of Engineering, Technology, Management and Research
A Peer Reviewed Open Access International Journal

sections. Analysis of the main sources is sufficient to understand the effect of AFDC hybrid control on losses.

The main sources of loss include the following: 1) transformer/resonant inductor loss (iron/winding loss); 2)MOSEFT conduction loss and switching loss; and 3) MOSFET body/rectifying diode conduction loss. The main components applied to the 3.3-kW prototype full-bridge series resonant dc–dc converter for loss analysis are summarized in Table II. Magnetic Component Losses: Transformer and inductor losses can be classified into two major categories: iron loss

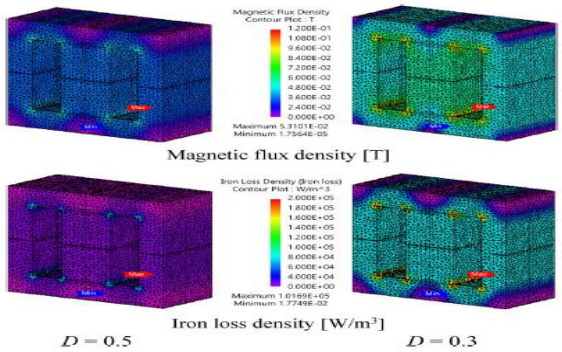

Fig. 8. Magnetic flux density and iron loss distribution of the transformer for Po = 300 W.

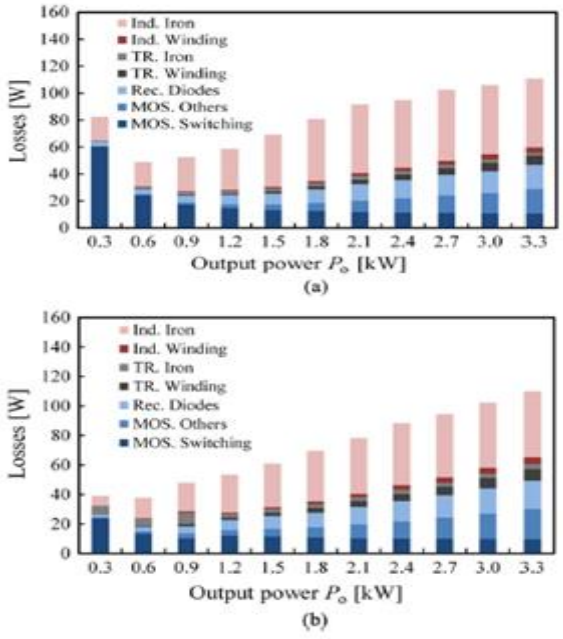

Fig. 9. Loss distributions versus Po. (a) Conventional frequency control. (b) AFDC hybrid control.

and winding loss. Among them, the winding loss considers the winding dc resistance. Skin effect losses can be prevented for the most part by utilizing Litz wire. Iron losses have a complex distribution because they depend on the magnetic flux density distribution that accounts for the core magnetic saturation. Moreover, the magnetic flube differently distributed unlike that by conventional frequency control with D = 0.5. Asymmetrical current can lead to partial core saturation; therefore, it is necessary to predict the distribution precisely. A magnetic field analysis simulation based on a finite-element method (FEM) using JMAG-Designer v11.1 is carried out to evaluate the complex magnetic flux distributions of the transformer and inductor core. The magnetic flux density and iron loss distributions of the transformer between D = 0.5 and D = 0.3 at Po = 300 W are presented in Fig. 8. As shown in Fig. 8, the value of the maximum flux density for D = 0.3 is about three times larger than that for D = 0.5, increasing the iron loss of the transformer. This is due to asymmetrical currents and higher harmonic frequencies.

Semiconductor Losses:

The switch conduction losses are calculated by the MOSFET approximation with the drain–source ON-state resistance. Because MOSFETs operate at ZVS conditions, only the turn-off loss is considered and not the turn-on loss. The conduction losses of the ant parallel diodes and the full-bridge rectifying diodes are calculated by using the diode approximation with the diode ON-state voltage under the zero-current condition, the diode ON-state resistance, and the diode current.

Efficiency Estimation:

The efficiency of the full-bridge series resonant dc–dc converter is predicted by using the loss results analyzed earlier. The loss distributions of conventional frequency control and AFDC hybrid control are compared in Fig. 9. Although AFDC hybrid control leads to increasing transformer losses, they comprise a small part of the total losses. On the other hand, because the switching frequency for conventional

ISSN No: 2348-4845
International Journal & Magazine of Engineering, Technology, Management and Research
A Peer Reviewed Open Access International Journal

frequency control is much higher than that of the proposed control, the converter suffers from increased switching loss and iron loss of the resonant inductor. These indicate that the MOSFETs and the inductor are the dominant sources of power losses.

Software Requirement

While coming to the software part here we are usingmatlab software which will be use to simulating the given code in blocks.

Block Diagram of VFD System

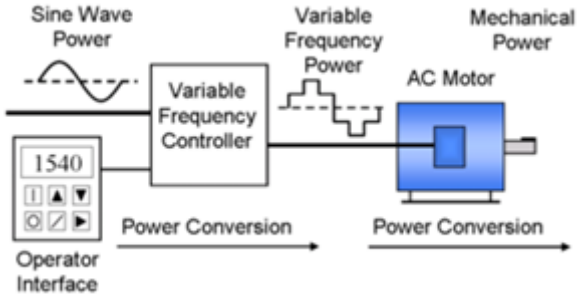

FIG: VFD System

4. Results:

Simulation Results

Electric Vehicle (1)

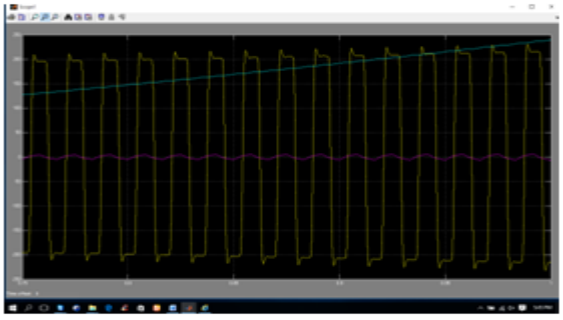

Electric Vehicle (2)

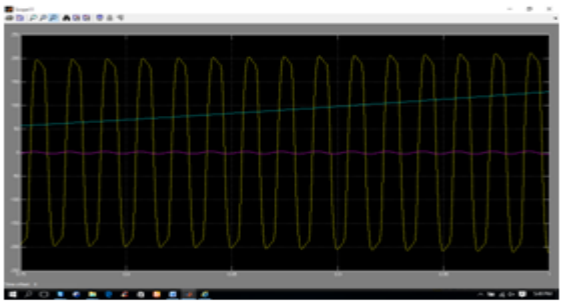

Electric Vehicle (3)

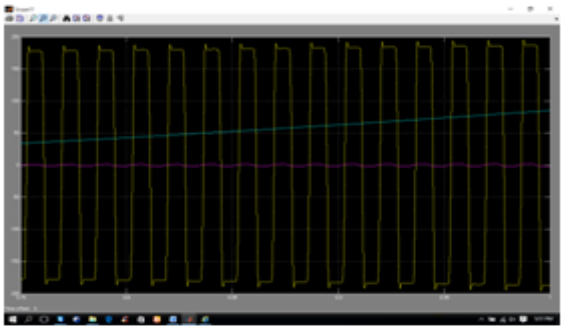

Electric vehicle (4)

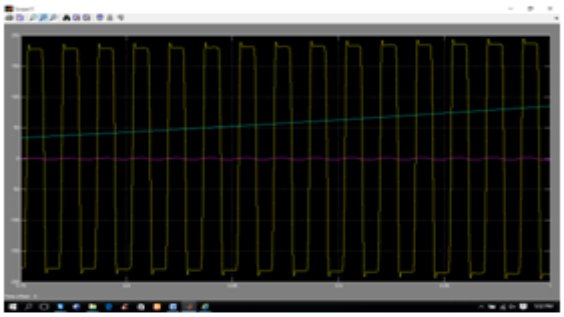

Conclusion:

An effective frequency modulation technique that adjusts the duty cycle for loads was proposed to increase the efficiency of the full-bridge series resonant dc–dc converter in the OBC for light loads. The optimum operation points allowing ZVS operation for a wide range of loads were theoretically analyzed in detail. To investigate the effect of AFDC hybrid control on the losses of the components, the losses of the primary components were calculated. In addition, the loss distributions of the magnetic components were estimated more precisely by utilizing a magnetic field analysis simulation tool based on a finite-element method (FEM). For verification of the proposed control method, the developed 3.3-kW full-bridge series resonant dc–dc converter was used. At different duty cycles, the experimental efficiency of the proposed method was compared with that of the conventional control method. The analytical and experimental results showed that the proposed control method improved the efficiency of the converter by a maximum of 4% for light loads without any extra hardware.

ISSN No: 2348-4845
International Journal & Magazine of Engineering, Technology, Management and Research
A Peer Reviewed Open Access International Journal

REFERENCES

[1] A. Kuperman, U. Levy, J. Goren, A. Zafransky, and A. Savernin, "Battery charger for electric vehicle traction battery switch station," IEEE Trans.Ind.Electron., vol. 60, no. 12, pp. 5391–5399, Dec. 2013.

[2] A. Hajimiragha, C. A. Cañizares, M. W. Fowler, and A. Elkamel, "Optimal transition to plug-in hybrid electric vehicles in Ontario, Canada, considering the electricity-grid limitations," IEEE Trans. Ind. Electron.,vol. 57, no. 2, pp. 690–701, Feb. 2010.

[3] M. Yilmaz and P. T. Krein, "Review of battery charger topologies, charging power levels, and infrastructure for plug-in electric and hybrid vehicles,"IEEE Trans. Power Electron., vol. 28, no. 5, pp. 2151–2169,May 2013.

[4] M. G. Egan, D. L. OSullivan, J. G. Hayes, M. J. Willers, and C. P. Henze, "Power-factor-corrected single-stage inductive charger for electric vehicle batteries," IEEE Trans. Ind. Electron., vol. 54, no. 2, pp. 1217–1226,Apr. 2007.

[5] J. Y. Lee and H. J. Chae, "6.6-kW onboard charger design using DCM PFC converter with harmonic modulation technique and two-stage DC/DC converter," IEEE Trans. Ind. Electron., vol. 61, no. 3, pp. 1243– 1252, Mar. 2014.

[6] B. Y. Chen and Y. S. Lai, "New digital-controlled technique for battery charger with constant current and voltage control without current feedback," IEEE Trans. Ind. Electron., vol. 59, no. 3, pp. 1545–1553,Mar. 2012.

[7] D. S. Gautam, F. Musavi, M. Edington, W. Eberle, and W. G. Dunford, "An automotive onboard 3.3-kW battery charger for PHEV application,"IEEE Trans. Veh. Technol., vol. 61, no. 8, pp. 3466–3474, Oct. 2012.

[8] D. Czarkowski and M. K. Kazimierczuk, "Single-capacitor phasecontrolled series resonant converter," IEEE Trans. Circuits Syst. I,Fundam. Theory Appl., vol. 40, no. 6, pp. 383–391, Jun. 1993.

[9] P. K. Jain, A. St-Martin, and G. Edwards, "Asymmetrical pulse-widthmodulated resonant DC/DC converter topologies," IEEE Trans. Power Electron., vol. 11, no. 3, pp. 413–422, May 1996.

[10] F. S. Pai, C. L. Ou, and S. J. Huang, "Plasma-driven system circuit design with asymmetrical pulsewidth modulation scheme," IEEE Trans. Ind.Electron., vol. 58, no. 9, pp. 4167–4174, Sep. 2011.

[11] B. C. Kim, K. B. Park, and G. W. Moon, "Asymmetric PWM control scheme during hold-up time for LLC resonant converter," IEEE Trans.Ind. Electron., vol. 59, no. 7, pp. 2992–2997, Jul. 2012.

[12] H. S. Kim, J. H. Jung, J. W. Baek, and H. J. Kim, "Analysis and design of a multioutput converter using asymmetrical PWM half-bridge flyback converter employing a parallel-series transformer," IEEE Trans. Ind. Electron.,vol. 60, no. 8, pp. 3115–3125, Aug. 2013.

Author Details:

A.Bhaktha Vachala received the B.Tech. degree from PBR VITS in the year 2003 and M.Tech degree from the JNTU, Hyderabad, India. Also Perusing Ph.D. degree from Jawaharlal Nehru Technological University, Hyderabad. He is working in the area of Electric vehicle applications in transportation systems from last four years. He has been with the Department of Electrical and Electronics Engineering, PBR Visvodaya Institute of Technology and Science, Kavali affiliated by JNTU Anatapur since last 10years, where he is currently an Associate Professor. His research interests include several areas of power electronics and electric vehicle applications of power electronics. He has authored or coauthored several papers in power

ISSN No: 2348-4845
International Journal & Magazine of Engineering, Technology, Management and Research
A Peer Reviewed Open Access International Journal

electronics. He holds a UGC sponsored project worth of 4,60,00/-.

S. Sai Krishna received the B.Tech degree from Sree Institute of Technical Education in the year 2012. And pursuing M.Tech in Visvodaya Engineering College in Kavali.